

Chain of nuclear spins system quantum computer taking into account second neighbor Ising spins interaction and numerical simulation of Shor factorization of $N=4$

G.V. López and L. Lara
Departamento de Física, Universidad de Guadalajara
Apartado Postal 4-137, 44410 Guadalajara, Jalisco, México

PACS: 03.67.Lx, 03.65.Ta

ABSTRACT

For a one-dimensional chain of four nuclear spins ($1/2$) and taking into account first and second neighbor interactions among the spin system, we make the numerical simulation of Shor prime factorization algorithm of the integer number $N = 4$ to study the influence of the second neighbor interaction on the performance of this algorithm. It is shown that the optimum Rabi's frequency to control the non-resonant effects is dominated by the second neighbor interaction coupling parameter (J'), and that a good Shor quantum factorization is achieved for a ratio of second to first coupling constant of $J'/J \geq 0.04$.

1. Introduction

The polynomial time solution of the prime decomposition of an integer number, given by Shor factorization algorithm [1] using quantum computation, has triggered the huge amount of work in quantum computers [2] and quantum information [3] areas in physics. This algorithm has already been demonstrated for few qubits [4] quantum computers. A qubit is the superposition of two quantum states of the system, say $|0\rangle$ and $|1\rangle$, $\Psi = C_0|0\rangle + C_1|1\rangle$ such that $|C_0|^2 + |C_1|^2 = 1$, and it is the basic element to process the information in a quantum computer. The states $|0\rangle$ and $|1\rangle$ can also be called basic qubits. The L -tensorial product of L -basic-qubits forms a register of length L , say $|x\rangle = |i_{L-1}, \dots, i_0\rangle$ with $i_j = 0, 1$ ("0" for the ground state and "1" for the excited state). The set of these states makes up the basis of the 2^L -dimensional Hilbert space where the quantum computer works, and a typical element of this space is given by $\Psi = \sum C_x|x\rangle$ with $\sum |C_x|^2 = 1$. A solid state quantum computer of our particular interest and which might be developed in a near future is using a one-dimensional chain of nuclear spins (1/2) which is inside a strong magnetic field in the z-direction and an rf-field in the x-y plane. The magnetic field in the z-direction determines the state of the nuclear spin, $|0\rangle$ if the nuclear spin is parallel to this magnetic field and $|1\rangle$ if the nuclear spin is in opposite direction. This magnetic field also determines the Zeeman spectrum of the system. The rf-field is used to cause the desired transitions between the Zeeman levels of the systems. Up to now, this model has been developed just theoretically and hopefully the technological and experimental part may start in a near future. However, because the Hamiltonian of this system is well known, very important theoretical studies have been made [5] which are also important for the general understanding of quantum computation [6]. In this model, first neighbor interaction among the nuclear spins is considered, and Shor quantum factorization of the number $N = 4$ has been simulated with this model [7]. In this paper, we consider also second neighbor interaction among the nuclear spins. Using this interaction, we study Shor factorization algorithm to factorize the integer number $N=4$, developing the proper code to do this. We study the well performance of this factorization through the fidelity parameter and determine the minimum value of the second neighbor interaction coupling constant to do this. Finally, we also point out the modification caused by the second neighbor interaction to the so called $2\pi k$ -method, used to suppress non-resonant transitions.

2. Equation of Motion

Consider a one-dimensional chain of four equally spaced nuclear-spins system (spin one half) making an angle $\cos \theta = 1/\sqrt{3}$ with respect the z-component of the magnetic field (chosen in this way to kill the dipole-dipole interaction between spins) and having an rf-magnetic field in the transversal plane. The magnetic field is given by

$$\mathbf{B} = (b \cos(\omega t + \varphi), -b \sin(\omega t + \varphi), B(z)) , \quad (1)$$

where b , ω and φ are the amplitude, the angular frequency and the phase of the rf-field, which could be different for different pulses. $B(z)$ is the amplitude of the z-component of the magnetic field. Thus, the Hamiltonian of the system up to second

neighbor interaction is given by

$$H = -\sum_{k=0}^3 \mu_{\mathbf{k}} \cdot \mathbf{B}_{\mathbf{k}} - 2J\hbar \sum_{k=0}^2 I_k^z I_{k+1}^z - 2J'\hbar \sum_{k=0}^1 I_k^z I_{k+2}^z , \quad (2)$$

where $\mu_{\mathbf{k}}$ represents the magnetic moment of the k th-nucleus which is given in terms of the nuclear spin as $\mu_{\mathbf{k}} = \hbar\gamma(I_k^x, I_k^y, I_k^z)$, being γ the proton gyromagnetic ratio. $\mathbf{B}_{\mathbf{k}}$ represents the magnetic field at the location of the k th-spin. The second term at the right side of (2) represents the first neighbor spin interaction, and the third term represents the second neighbor spin interaction. J and J' are the coupling constants for these interactions. This Hamiltonian can be written in the following way

$$H = H_0 + W , \quad (3a)$$

where H_0 and W are given by

$$H_0 = -\hbar \left\{ \sum_{k=0}^3 \omega_k I_k^z + 2J(I_0^z I_1^z + I_1^z I_2^z + I_2^z I_3^z) + 2J'(I_0^z I_2^z + I_1^z I_3^z) \right\} \quad (3b)$$

and

$$W = -\frac{\hbar\Omega}{2} \sum_{k=0}^3 \left[e^{i\omega t} I_k^+ + e^{-i\omega t} I_k^- \right] . \quad (3c)$$

The term ω_k represents the Larmore frequency of the k th-spin, $\omega_k = \gamma B(z_k)$. The term Ω is the Rabi's frequency, $\Omega = \gamma b$. Finally, the term $I_k^{\pm} = I_k^x \pm iI_k^y$ represents the ascend operator (+) or the descend operator (-). The Hamiltonian H_0 is diagonal on the basis $\{|i_3 i_2 i_1 i_0\rangle\}$, where $i_j = 0, 1$ (zero for the ground state and one for the exited state),

$$H_0|i_3 i_2 i_1 i_0\rangle = E_{i_3 i_2 i_1 i_0} |i_3 i_2 i_1 i_0\rangle . \quad (4a)$$

The eigenvalues $E_{i_3 i_2 i_1 i_0}$ are given by

$$E_{i_3 i_2 i_1 i_0} = -\frac{\hbar}{2} \left\{ \sum_{k=0}^3 (-1)^{i_k} \omega_k + J \sum_{k=0}^2 (-1)^{i_k + i_{k+1}} + J' \sum_{k=0}^1 (-1)^{i_k + i_{k+2}} \right\} . \quad (4b)$$

The term (3c) of the Hamiltonian allows to have a single spin transitions on the above eigenstates by choosing the proper resonant frequency.

To solve the Schrödinger equation

$$i\hbar \frac{\partial \Psi}{\partial t} = H\Psi , \quad (5)$$

let us propose a solution of the form

$$\Psi(t) = \sum_{k=0}^{15} C_k(t) |k\rangle , \quad (6)$$

where we have used decimal notation for the eigenstates in (4a), $H_0|k\rangle = E_k|k\rangle$. Substituting (6) in (5), multiplying for the bra $\langle m|$, and using the orthogonality relation $\langle m|k\rangle = \delta_{mk}$, we get the following equation for the coefficients

$$i\hbar \dot{C}_m = E_m C_m + \sum_{k=0}^{15} C_k \langle m|W|k\rangle \quad m = 0, \dots, 15. \quad (7)$$

Now, using the following transformation

$$C_m = D_m e^{-iE_m t/\hbar} , \quad (8)$$

the fast oscillation term $E_m C_m$ of Eq. (7) is removed (this is equivalent to go to the interaction representation), and the following equation is gotten for the coefficients D_m

$$i\dot{D}_m = \frac{1}{\hbar} \sum_{k=0}^{15} W_{mk} D_k e^{i\omega_{mk} t} , \quad (9a)$$

where W_{mk} denotes the matrix elements $\langle m|W|k\rangle$, and ω_{mk} are defined as

$$\omega_{mk} = \frac{E_m - E_k}{\hbar} . \quad (9b)$$

Eq. (9a) represents a set of 32 real coupling ordinary differential equations which can be solved numerically, and where W_{mk} are given by

$$W_{mk} = -\frac{\hbar\Omega}{2} \times (0, \quad z \text{ "or"} \quad z^*) , \quad (9c)$$

where z is defined as $z = e^{i(\omega t + \varphi)}$, and z^* is its complex conjugated.

3. Shor's factorization algorithm and numerical simulation

Following Shor's approach to get the factorization of an integer number N , one selects a $L + M$ -register of the form $|x; y\rangle$, where $|x\rangle$ is the input register of length L , and $|y\rangle$ is the valuation register of length M . The $|y\rangle$ register will store the values of the periodic function $y(x) = q^x \pmod{N}$, where the integer q is a coprime number of N , that is, their grater common divisor is one ($\gcd(q, N) = 1$). Thus, starting with the ground state,

$$\Psi_0 = |0; 0\rangle , \quad (10)$$

the uniform superposition state is created in the x-register,

$$\Psi_1 = \frac{1}{2^{L/2}} \sum_x |x; 0\rangle , \quad (11)$$

where 2^L is the number of qubits in the x-register. On the next step, the computation of the function $y(x) = q^x \pmod{N}$ is carried out in the y-register,

$$\Psi_2 = \frac{1}{2^{L/2}} \sum_x |x; y(x)\rangle . \quad (12)$$

Then, the discrete Fourier transformation is done in the x-register,

$$\Psi_3 = \frac{1}{2^L} \sum_x \sum_k e^{i2\pi kx/2^L} |x; y(x)\rangle . \quad (13)$$

After these steps, one makes the measurement of the state on the x-register, and the probability must be a peak distribution with peaks separation, Δx , equal to $\Delta x = 2^L/T$, whenever 2^L be divisible by the period T . In this way, one finds the

period T of the function $y(x) = q^x \pmod N$. If this period is an even number, the factors of N can be computed finding the greatest common divisor of $q^{T/2} \pm 1$ and the number N ($\gcd(q^{T/2} \pm 1, N)$).

Now, for $N = 4$, one just needs two-qubits registers in the x-register ($L = 2$) and two-qubits registers in the y-register ($M = 2$). The only coprime number is $q = 3$, and the function $y(x) = 3^x \pmod 4$ has period $T = 2$. Therefore, starting with the function

$$\Psi_0 = |00; 00\rangle , \quad (14a)$$

the superposition state is created in the x-register,

$$\Psi_1 = \frac{1}{2} \left\{ |00; 00\rangle + |01; 00\rangle + |10; 00\rangle + |11; 00\rangle \right\} . \quad (14b)$$

Next, the function $y(x) = 3^x \pmod 4$ is valuated on the y-register,

$$\Psi_2 = \frac{1}{2} \left\{ |00; 01\rangle + |01; 11\rangle + |10; 01\rangle + |11; 11\rangle \right\} . \quad (14c)$$

Then, the discrete Fourier transformation is performed to get (after summation of all terms) the wave function

$$\Psi_3 = \frac{1}{2} \left\{ |00; 01\rangle + |00; 11\rangle + |10; 01\rangle + |10; 11\rangle \right\} . \quad (14d)$$

The measurement on the x-register give us the states $|00\rangle$ or $|10\rangle$ ($x = 0$ or $x = 2$). So, one has $\Delta x = 2$, and the period of our function is $T = 2^2/2 = 2$. Finally, the factors of $N = 4$ ($4 = 2 \cdot 2$) are obtained from $\gcd(3^{T/2} - 1, 4) = 2$.

To make the numerical simulation of this algorithm, we have chosen the following parameters in units of $2\pi \times \text{Mhz}$,

$$\omega_0 = 100 , \omega_1 = 200 , \omega_2 = 400 , \omega_3 = 800 , J = 10 , J' = 0.4 , \Omega = 0.1 . \quad (15)$$

These parameters were chosen in this way to have a clear separation on the Zeeman spectrum and to have a good definition for the resonant transitions in our numerical simulation. This does not imply a restriction on our simulations since our main results are applicable also to the current design [6]. Now, starting with the ground state of the system, $|0000\rangle$, we create a superposition state in the x-register using three $\pi/2$ -pulses with zero phases and with resonant frequencies $\omega_{0,4}$, $\omega_{0,8}$ and $\omega_{4,12}$. The valuation of the function $y(x) = 3^x \pmod 4$ in the y-register is carried out with four π -pulses with zero phases and with the resonant frequencies $\omega_{0,1}$, $\omega_{4,5}$, $\omega_{5,7}$ and $\omega_{13,15}$. Finally, the discrete Fourier transformation in the x-register is gotten through five π -pulses with zero phases and with the frequencies $\omega_{6,7}$, $\omega_{2,6}$, $\omega_{2,3}$, $\omega_{14,15}$, and $\omega_{11,15}$. The transitions involved in the algorithm are shown in Fig. 1. Note that at the end of Shor's algorithm, one must get the following probabilities

$$|C_1|^2 = |C_3|^2 = |C_9|^2 = |C_{11}|^2 = 1/4 , \quad (16)$$

according with our final wave function (14d), note from (8) that $|C_k| = |D_k|$. Fig. 2 shows the behavior of the probabilities $|C_k|^2$ during the entire Shor's algorithm. Fig. 2a shows the formation of the superposition state (14b), starting from the ground

state (14a). Fig. 2b shows the valuation of the function $y(x) = 3^x(\text{mod } 4)$ at the end of four π -pulses, wave function (14c). Fig. 2c shows the formation of the wave function (14d) at the end of five π -pulses. To better illustrate what is happening during the Shor's algorithm, we calculated the expected values of the z-component of the spin of the system for each qubit. These expected values are given by

$$\langle I_0^z \rangle = \frac{1}{2} \sum_{k=0}^{15} (-1)^k |C_k(t)|^2, \quad (17a)$$

$$\begin{aligned} \langle I_1^z \rangle = \frac{1}{2} & \left\{ |C_0|^2 + |C_1|^2 - |C_2|^2 - |C_3|^2 + |C_4|^2 + |C_5|^2 - |C_6|^2 - |C_7|^2 \right. \\ & \left. + |C_8|^2 + |C_9|^2 - |C_{10}|^2 - |C_{11}|^2 + |C_{12}|^2 + |C_{13}|^2 - |C_{14}|^2 - |C_{15}|^2 \right\}, \end{aligned} \quad (17b)$$

$$\begin{aligned} \langle I_2^z \rangle = \frac{1}{2} & \left\{ |C_0|^2 + |C_1|^2 + |C_2|^2 + |C_3|^2 - |C_4|^2 - |C_5|^2 - |C_6|^2 - |C_7|^2 \right. \\ & \left. + |C_8|^2 + |C_9|^2 + |C_{10}|^2 + |C_{11}|^2 - |C_{12}|^2 - |C_{13}|^2 - |C_{14}|^2 - |C_{15}|^2 \right\}, \end{aligned} \quad (17c)$$

and

$$\langle I_3^z \rangle = \frac{1}{2} \sum_{k=0}^7 |C_k|^2 - \frac{1}{2} \sum_{k=8}^{15} |C_k|^2. \quad (17d)$$

Fig. 3a shows these expected values during the formation of the superposition state on the x-register. Fig. 3b shows their behavior during the valuation of the function $y(x) = 3^x(\text{mod } 4)$ on the y-register, and Fig. 3c shows their behavior during the creation of the discrete Fourier transformation. Of course, this observed behavior is the behavior that one could have expected from the Shor's algorithm. Fig. 4a shows the probabilities of the expected four-qubits registers at the end of Shor's algorithm (wave function (14d)), and Fig. 4b shows the probabilities of the non-resonant states.

To determine the value of the second neighbor coupling constant needed to have a good reproduction of the Shor's algorithm, we calculate the fidelity parameter [8],

$$F = \langle \Psi_{\text{expected}} | \Psi \rangle, \quad (18)$$

where Ψ_{expected} is the wave function (14d), and Ψ is the resulting wave function from our computer simulation. This is done as a function of the ratio J'/J (second to first neighbor coupling constant interactions). Fig. 5 shows our results of the calculation of this parameter as a function of J'/J . As one can see, for a value of $J'/J \geq 0.04$, one can say that we have already a very good reproduction of the Shor factorization algorithm. Of course, this does not mean that second neighbor

interaction is needed to implement Shor quantum algorithm since, if $J' = 0$, one can just change the protocol (resonant pulses) to get this algorithm. Rather, what this result means is that, in the case of having second neighbor interaction ($J' \neq 0$), the optimum performance of our Shor quantum algorithm is gotten for the above ratio.

4. Second neighbor interaction and the $2\pi k$ -method

One of the important results from the consideration of first neighbor interaction and the selection of the parameter as $J/\Delta\omega \ll 1$ and $\Omega/\Delta\omega \ll 1$ is the possibility of choosing the Rabi's frequency Ω in such a way that the non-resonant effects are eliminated. This procedure is called the $2\pi k$ -method [9], and this Rabi's frequency for a π -pulse is chosen as $\Omega = |\Delta|/\sqrt{4k^2 - 1}$, where k is an integer number, and Δ is the detuning parameter between the states $|p\rangle$ and $|m\rangle$, $\Delta = (E_p - E_m)/\hbar - \omega$ being ω the electromagnetic resonant frequency. This detuning parameter is proportional to the first neighbor coupling constant J . Let us see how this detuning parameter is modified due to second neighbor interaction. Assuming that the states $|p\rangle$ and $|m\rangle$ are the only ones involved in the dynamics, from Eq. (9a), one has

$$i\dot{D}_m = \frac{W_{mp}}{\hbar} D_p e^{i\omega_{mp}t}, \quad \text{and} \quad i\dot{D}_p = \frac{W_{pm}}{\hbar} D_m e^{i\omega_{pm}t}. \quad (19)$$

Thus, given the initial conditions $D_p(0) = C_p(0)$ and $D_m(0) = C_m(0)$, the solution is readily given by

$$D_p(t) = \left\{ C_p(0) \left[\cos \frac{\Omega_e t}{2} - i \frac{\Delta}{\Omega_e} \sin \frac{\Omega_e t}{2} \right] + i \frac{\Omega C_m(0)}{\Omega_e} \sin \frac{\Omega_e t}{2} \right\} e^{\frac{i\Delta t}{2}} \quad (20a)$$

and

$$D_m(t) = \left\{ C_m(0) \left[\cos \frac{\Omega_e t}{2} - i \frac{\Delta}{\Omega_e} \sin \frac{\Omega_e t}{2} \right] + i \frac{\Omega C_p(0)}{\Omega_e} \sin \frac{\Omega_e t}{2} \right\} e^{-\frac{i\Delta t}{2}}, \quad (20b)$$

where Ω_e is defined as $\Omega_e = \sqrt{\Omega^2 + \Delta^2}$. So, for example, at the end of a π -pulse ($t = \tau = \pi/\Omega$), the argument of the periodic functions in (20a) and (20b) is given by $\Omega_e \pi/2\Omega$. If one makes this term to be equal to any multiple of π , one can get rid of the non-resonant terms since the solutions are given by

$$D_p(\tau) = (-1)^k C_p(0) e^{i\Delta\pi/2\Omega}, \quad \text{and} \quad D_m(\tau) = (-1)^k C_m(0) e^{-i\Delta\pi/2\Omega}.$$

The Rabi's frequency obtained from the condition $\Omega_e \pi/2\Omega = k\pi$ is given by $\Omega = |\Delta|/\sqrt{4k^2 - 1}$, and this is the so called $2\pi k$ -method.

Now, let us select a resonant transition containing the Larmore frequency ω_0 . These frequencies could be $\omega_0 + J + J'$, $\omega_0 - J + J'$, $\omega_0 - J - J'$ or $\omega_0 + J - J'$ which correspond to the transitions (decimal notation) $|0\rangle \leftrightarrow |1\rangle$ ($|10\rangle \leftrightarrow |11\rangle$), $|2\rangle \leftrightarrow |3\rangle$, $|6\rangle \leftrightarrow |7\rangle$, and $|2\rangle \leftrightarrow |3\rangle$. So, all of these states are pertubated during a pulse, and the frequency difference Δ may have the values $2J$, $2J'$, $2J + 2J'$, or $2J - 2J'$. Choosing other Larmore frequencies, the additional values for the detuning parameter are $4J$, and $4J + 2J'$. Thus, denoting by $\Omega_\Delta^{(k)}$ the Rabi's frequency selected by this method,

$$\Omega_\Delta^{(k)} = \frac{|\Delta|}{\sqrt{4k^2 - 1}}, \quad (21)$$

there are five possible values for Δ which are $4J + 2J'$, $4J$, $2J + 2J'$, $2J$ and $2J'$.

To see the dependence of the Shor's algorithm with respect the Rabi's frequency, we use again the fidelity parameter parameter (18). Using the same values for our parameters as (15) but Ω , Fig. 6 shows the fidelity parameter as a function of the Rabi's frequency. The lines $L1$, $L2$ and $L3$ mark the Ω 's values where this fidelity has peaks. These peaks correspond to the following $2\pi k$ -method Rabi frequencies

$$\begin{aligned}\Omega_{4J+2J'}^{(252)} &\approx \Omega_{4J}^{(250)} \approx \Omega_{2J+2J'}^{(129)} \approx \Omega_{2J}^{(124)} \approx \Omega_{2J'}^{(5)} = 0.080403 , \\ \Omega_{4J+2J'}^{(202)} &\approx \Omega_{4J}^{(198)} \approx \Omega_{2J+2J'}^{(103)} \approx \Omega_{2J}^{(98)} \approx \Omega_{2J'}^{(4)} = 0.100791 ,\end{aligned}$$

and

$$\Omega_{4J+2J'}^{(150)} \approx \Omega_{4J}^{(147)} \approx \Omega_{2J+2J'}^{(76)} \approx \Omega_{2J}^{(73)} \approx \Omega_{2J'}^{(3)} = 0.135225 .$$

As one can see in Fig. 7, where we have plotted $\Omega_{\Delta}^{(k)}$ (for the detuning values mentioned above) and where the lines $L1$, $L2$ and $L3$ have been drawn, around these lines there are several other values of $\Omega_{4J+2J'}^{(k)}$, $\Omega_{4J}^{(k)}$, $\Omega_{2J+2J'}^{(k)}$ and $\Omega_{2J}^{(k)}$ which, in principle, should cause a peak in the fidelity parameter (because they belong to the $2\pi k$ -method). However, they do not appear at all on Fig. 6. This means that the peaks values on the fidelity parameter are fully dominated by the second neighbor coupling interaction parameter (J').

5. Conclusions

For a one-dimensional chain of nuclear spins (one half) system quantum computer, we have considered first and second neighbor interactions, and we have study the effects of second neighbor interaction on Shor quantum factorization algorithm of the number $N = 4$. We have shown that a good factorization algorithm can be gotten if the ratio of second to first neighbor interaction constants is chosen such that $J'/J \geq 0.04$. We have shown also that the application of $2\pi k$ -method to eliminate non-resonant transitions is not so simple since the detuning factor varies with both parameters J and J' (first and second neighbor coupling interactions). However, the peaks on the fidelity parameter are dominated by the second neighbor coupling parameter. In other words, if there exists second neighbor interaction in a chain of nuclear spin system quantum computer, this interaction may dominate the $2\pi k$ -method to control non-resonant effects.

Acknowledgements

This work was supported by SEP under the contract PROMEP/103.5/04/1911 and the University of Guadalajara.

Figure Captions

Fig. 1 Energy levels and resonant frequencies used within the algorithm.

Fig. 2 Probabilities $|C_k|^2 : (k)$. (a) Formation of superposition state in the x-register, wave function (14b). (b) Formation of the wave function (14c). (c) Formation the wave function (14d).

Fig. 3 Expected values $\langle I_k^z \rangle$: (k=0,1,2,3). (a) During formation of wave function (14b). (b) During formation of the wave function (14c). (c) During formation of the wave function (14d).

Fig. 4 Probabilities $|C_k|^2$. (a) For the expected states $k = 1, 3, 5, 7$. (b) For the non-resonant states $k = 0, 2, 4, 6, 8, 9, 10, 11, 12, 13, 14, 15$.

Fig. 5 Fidelity parameter as a function of J'/J .

Fig. 6 Fidelity parameter as a function of Ω .

Fig. 7 Rabi frequency $\Omega_{\Delta}^{(k)}$ as a function of k for $\Delta = 4J + 2J'$ (1), $\Delta = 4J$ (2), $\Delta = 2J + 2J'$ (3), $\Delta = 2J$ (4), $\Delta = 2J'$ (5). Lines $L1$, $L2$ and $L3$ correspond to Fig. 6.

References

1. P.W. Shor, *Proc. of the 35th Annual Symposium on the Foundation of the Computer Science*, IEEE, Computer Society Press, N.Y. 1994, 124.
P.W. Shor, *Phys. Rev. A* **52** (1995) R2493.
2. C. Williams and S. Clearwater, *Exploration in Quantum Computing*, Springer-Verlag, Berlin, 1995.
3. M.A. Nielsen and I.L. Chuang, *Quantum Computation and Quantum Information*, Cambridge University Press, 2000.
4. D. Boshi, S. Branca, F.D. Martini, L. Hardy, and S. Popescu
Phys. Rev. Lett., **80** (1998) 1121.
C.H. Bennett and G. Brassard, *Proc. IEEE international Conference on Computers, Systems, and Signal Processing*, N.Y. (1984) 175.
I.L. Chuang, N.Gershenfeld, M.G. Kubinec, and D.W. Lung
Proc. R. Soc. London A, **454** (1998) 447.
I.L. Chuang, N. Gershenfeld, and M.G. Kubinec
Phys. Rev. Lett., **18** (1998) 3408.
I.L. Chuang, L.M.K. Vandersypen, X.L. Zhou, D.W. Leung, and S. Lloyd,
Nature, **393** (1998) 143.
P.Domokos, J.M. Raimond, M. Brune, and S. Haroche,
Phys. Rev. Lett., **52** (1995) 3554.
J.Q. You, Y. Nakamura, F.Nori, *Phys. Rev. Lett.*,**91** (2002) 197902.
L.M.K. Vandersypen, M. Steffen, G. Breyta, C.S. Yannoni, M.H. Sherwood
and I.L. Chuang, *Nature*, **414** (2001) 883.
5. G.P. Berman, G.D. Doolen, D.D. Holm and V.I. Tsifrinovich,
Phys. Lett. A **193** (1994) 444.
6. G.P. Berman, G.D. Doolen, D.I. Kamenev, G.V. López, and
V.I. Tsifrinovich, *Phys. Rev. A* **6106** (2000) 2305.
7. G.P. Berman, G.D. Doolen, G.V. López, and V.I. Tsifrinovich
quant-ph/9909027 (1999).
8. A. Peres, *Phys. Rev. A* **30** (1984) 1610.
B. Schumacher, *Phys. Rev. A*,**51** (1995) 2738.
9. G.P. Berman, G.D. Doolen, D.I. Kamenev, G.V. López and V.I. Tsifrinovich
Contemporary Mathematics, **305** (2002) 13.

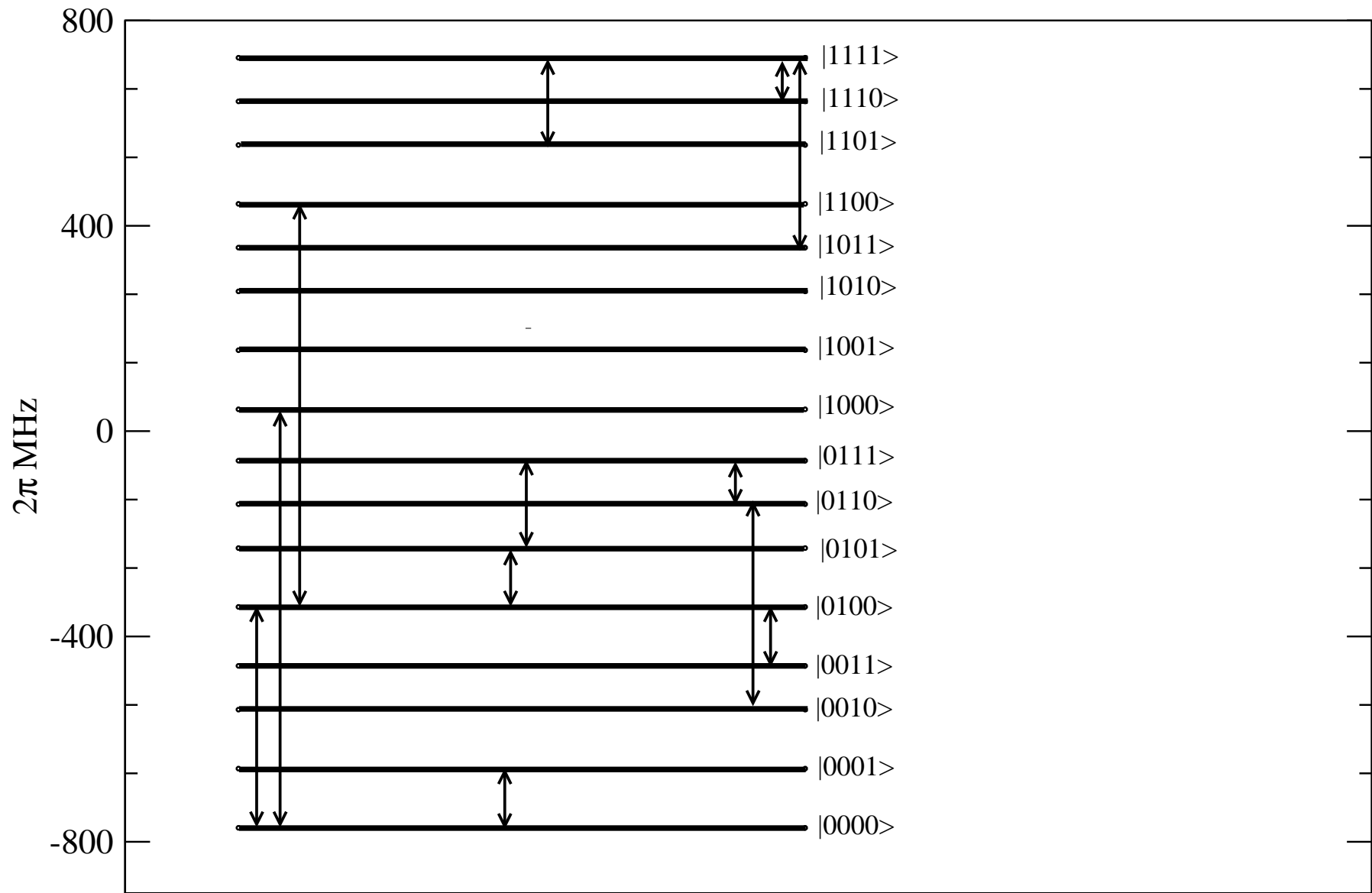


Fig. 1

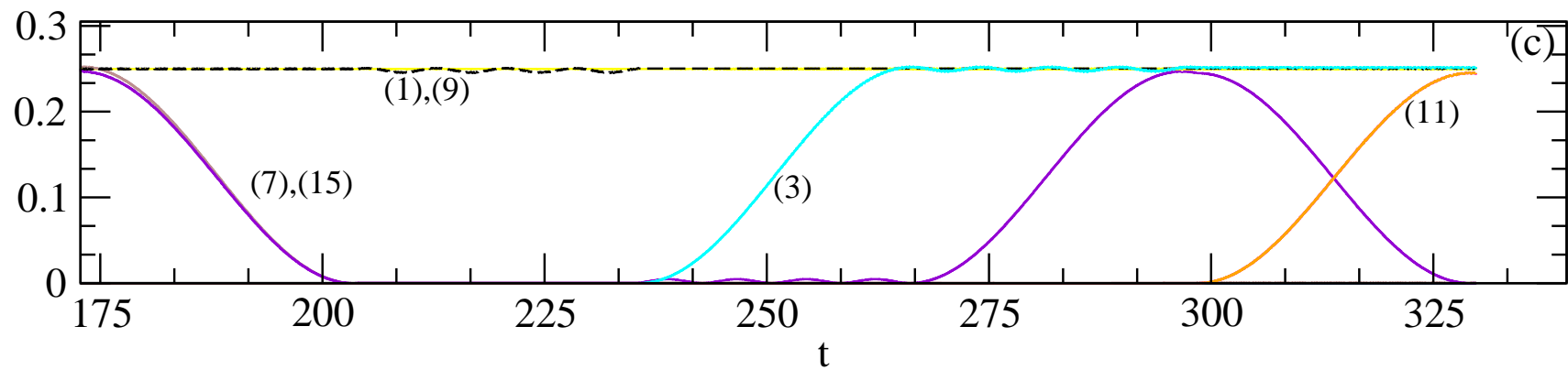
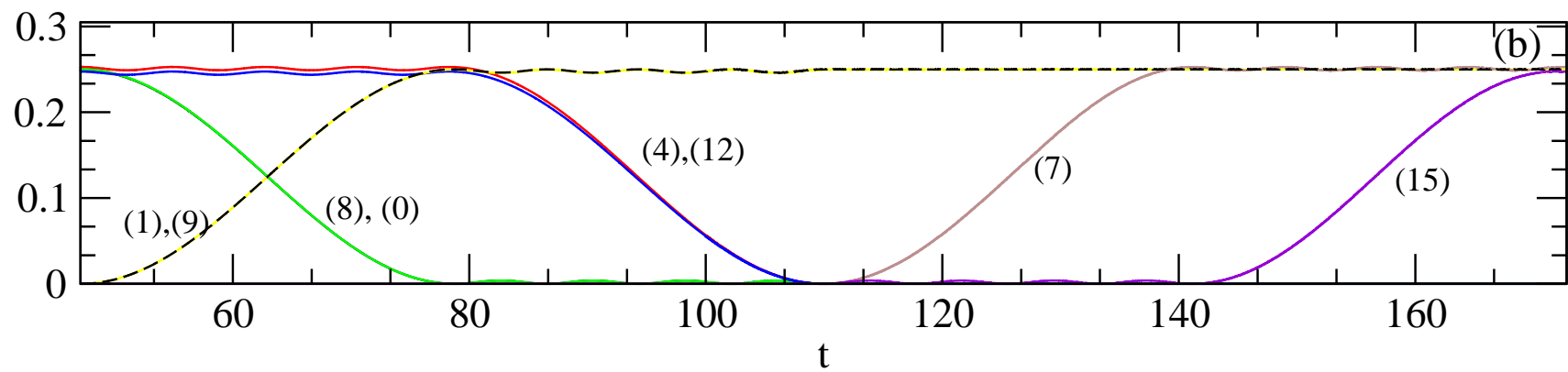
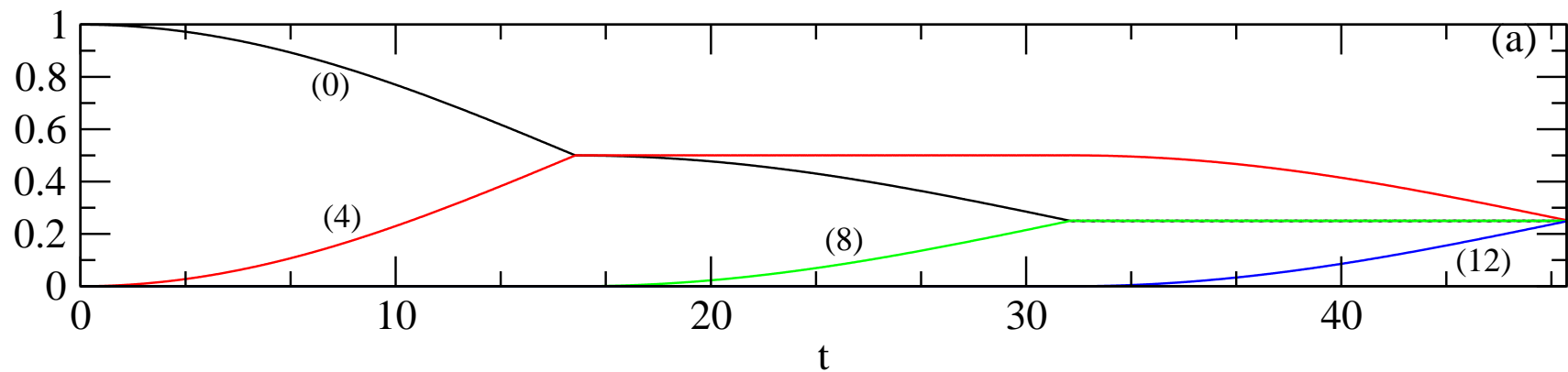


Fig. 2

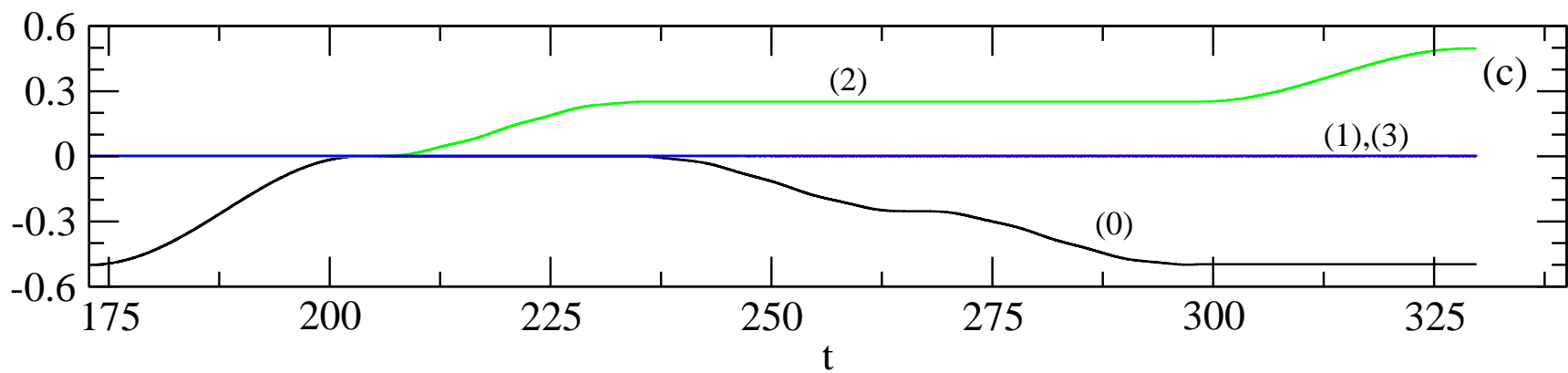
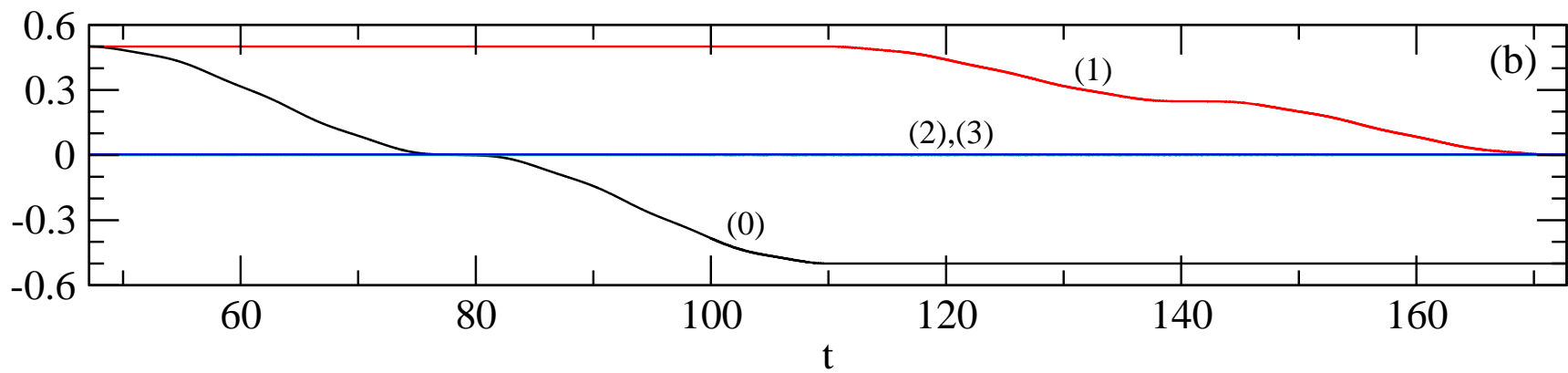
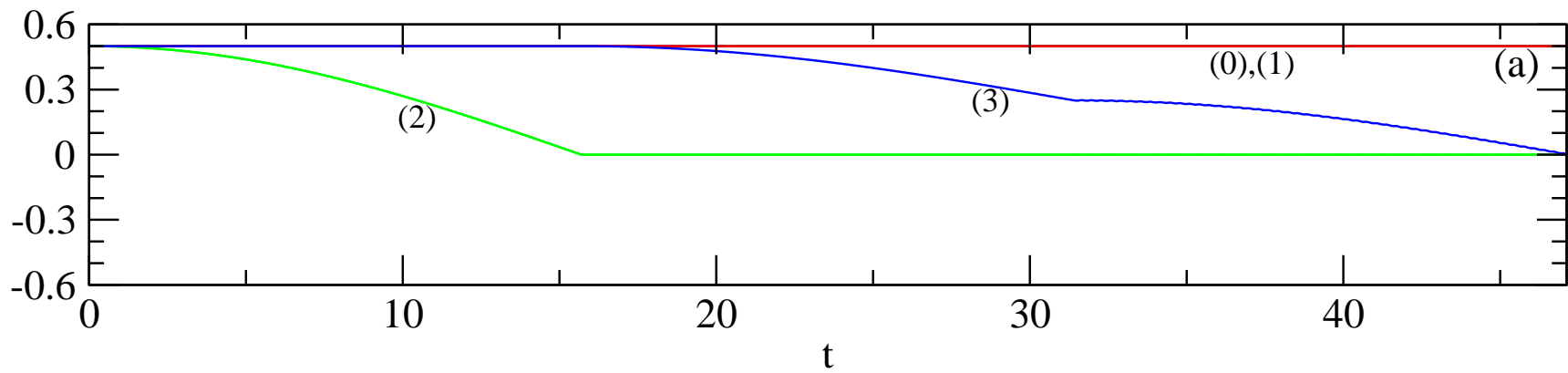


Fig. 3

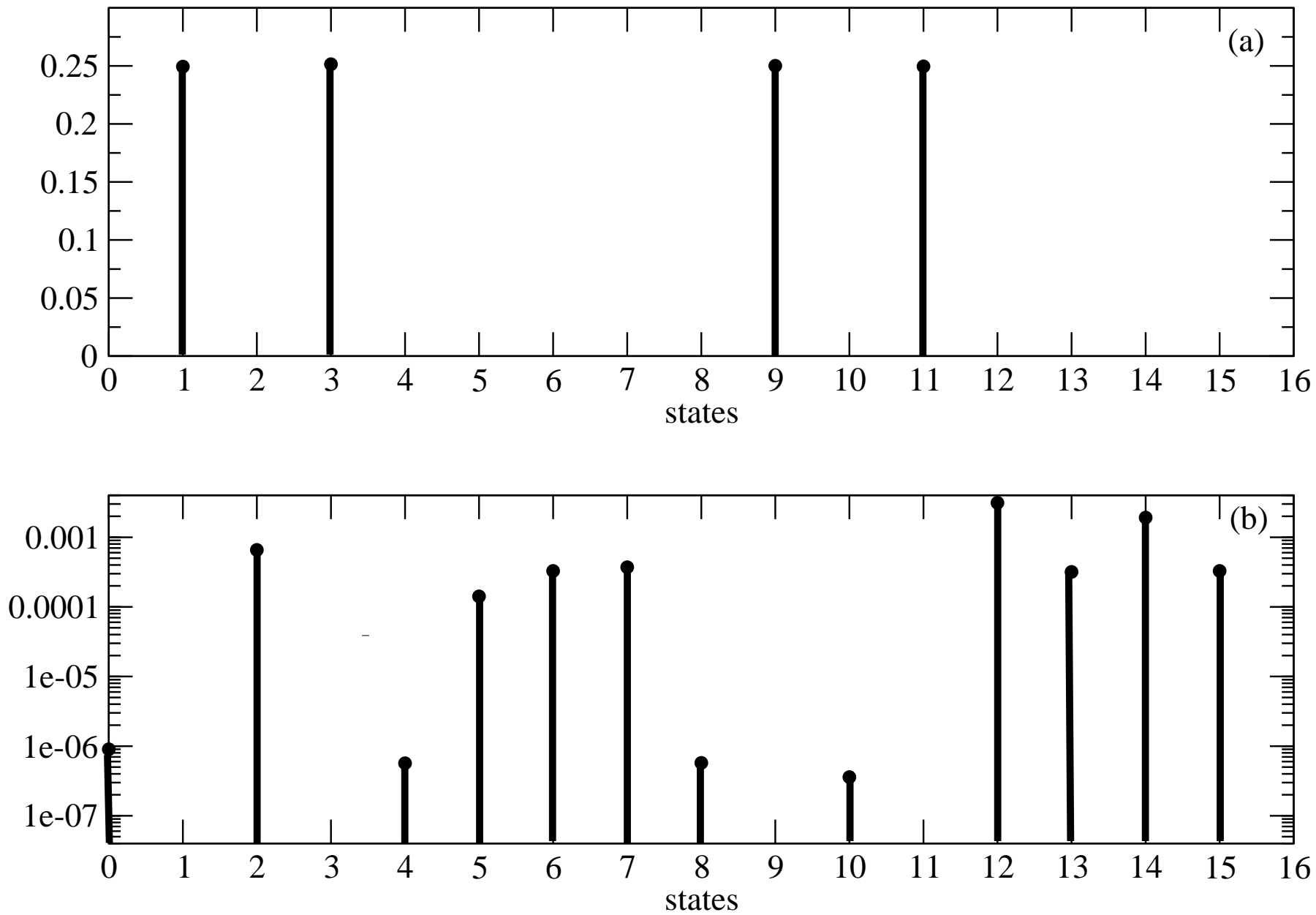


Fig. 4

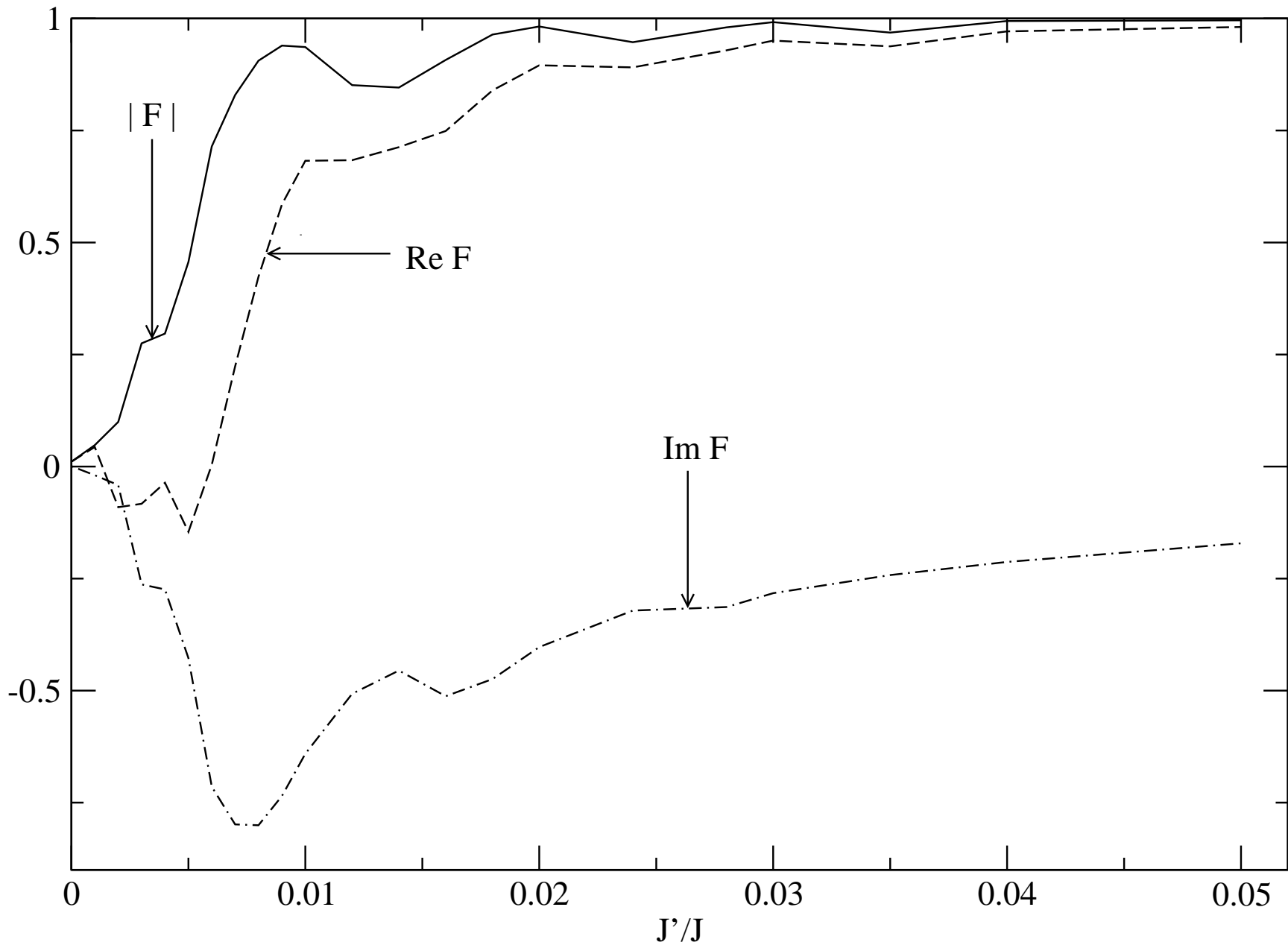


Fig. 5

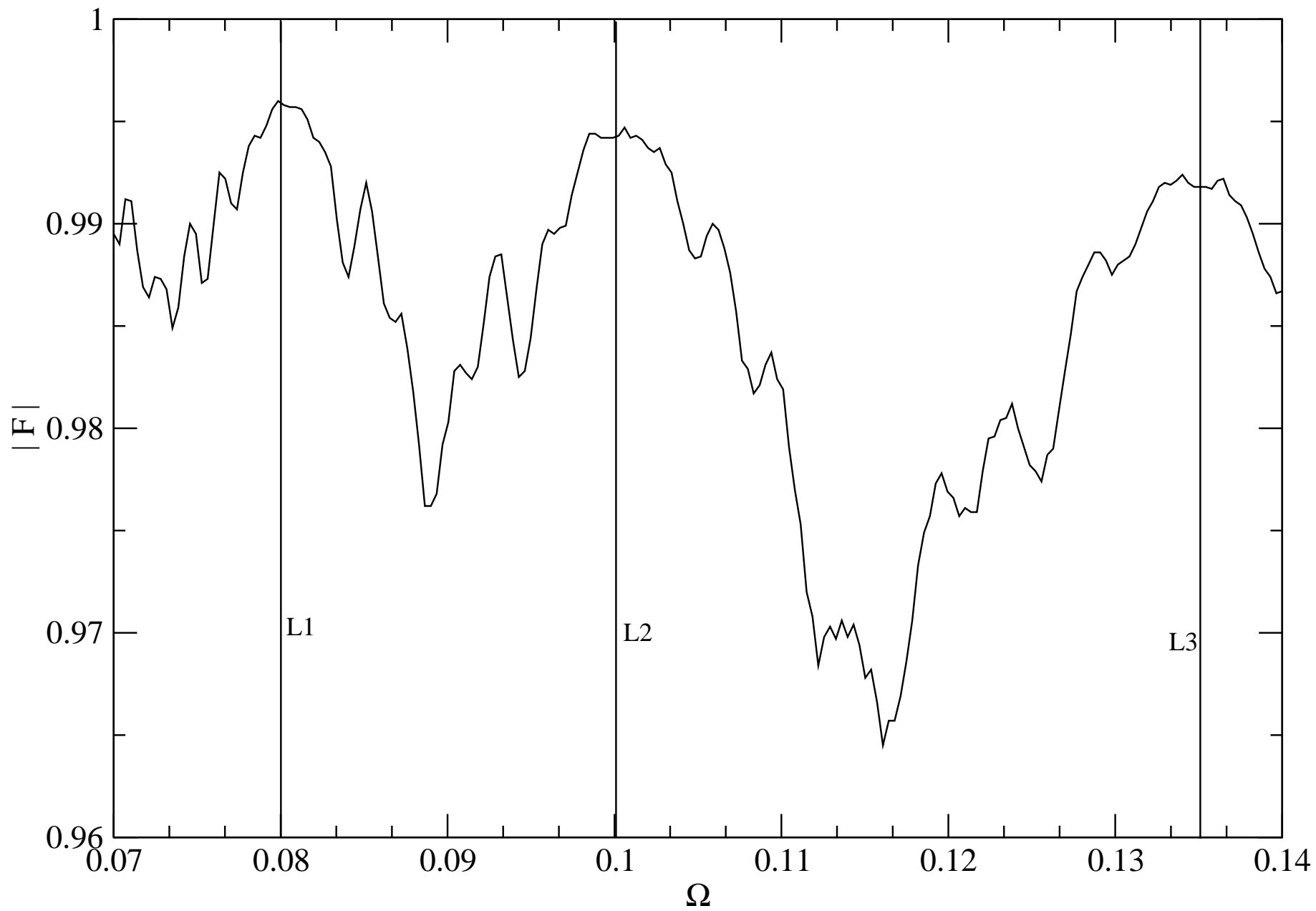


Fig. 6

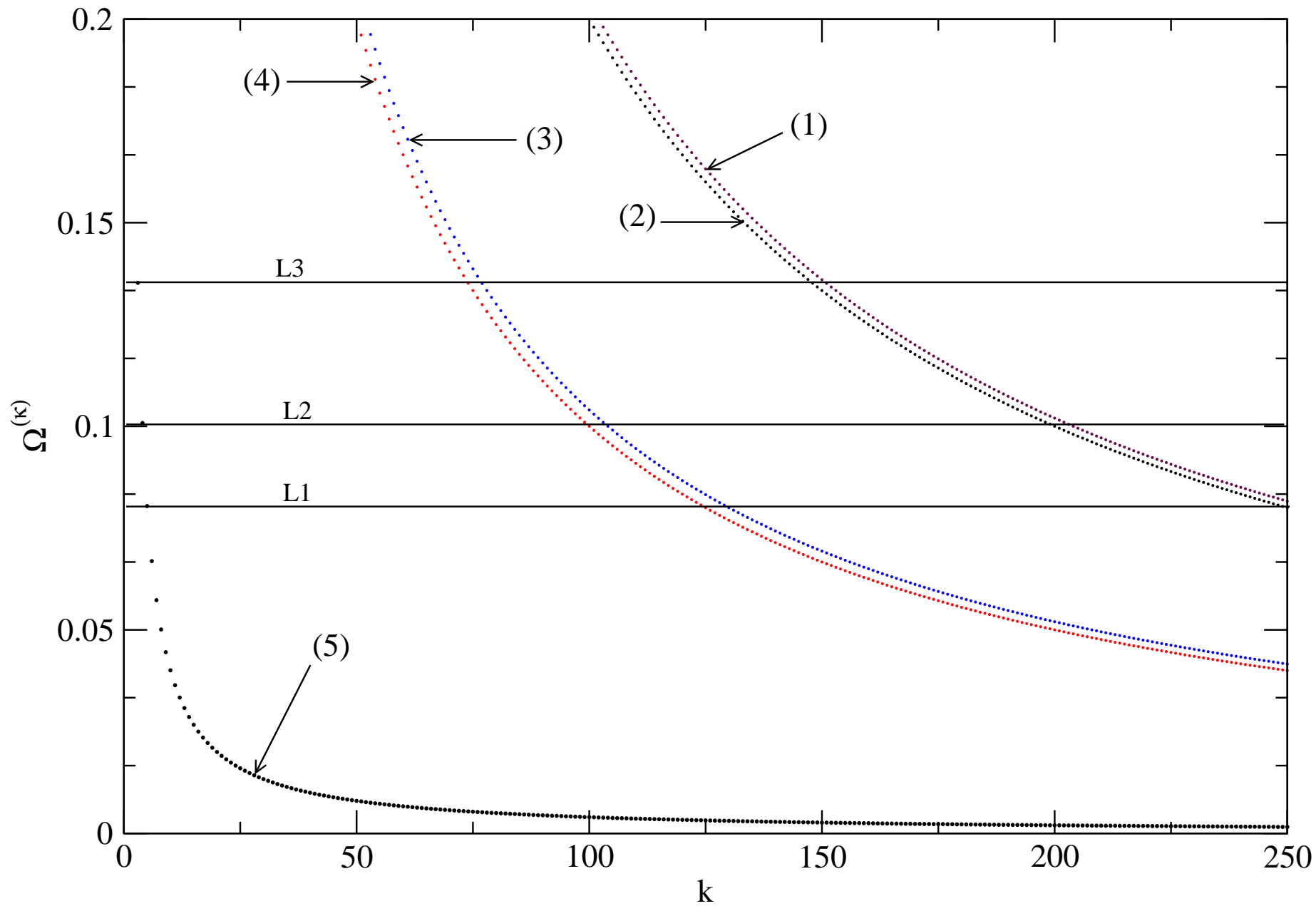


Fig. 7